Supramolecular Chemistry

International Edition: DOI: 10.1002/anie.201501507
German Edition: DOI: 10.1002/ange.201501507

Facile Self-Assembly of Metallo-Supramolecular Ring-in-Ring and Spiderweb Structures Using Multivalent Terpyridine Ligands**

*Jun-Hao Fu, Yin-Hsuan Lee, Yun-Jui He, and Yi-Tsu Chan**

Abstract: *A series of metallo-supramolecular ring-in-ring structures was generated by assembling Cd^{II} ions and the multivalent terpyridine ligands (**L**$^{1\text{-}3}$) composed of one 60°-bent and two 120°-bent bis(terpyridine)s with varying alkyl linker lengths. The mechanistic study for the self-assembly process excluded an entropically templated pathway and showed that the intramolecularly complexed species is the key intermediate leading to ring-in-ring formation. The next-generation superstructure, a spiderweb, was produced in quantitative yield using the elongated decakis(terpyridine) ligand (**L**^{5}).*

Precise self-assembly of desired supramolecular architectures has great importance in chemistry, biology, and materials science owing to the capability of controlling higher-order domain structures for potential applications in catalysis, drug delivery, electronics, and so on.[1] Coordination-driven self-assembly is one of the most promising strategies for preparing a wide variety of pre-designable structures, such as polygons,[2] fractals,[3] polyhedra,[2a,b,4] helicates,[5] or catenanes,[6] through a proper combination of ligand geometry and directional coordinative interactions under either kinetic or thermodynamic control. Among these aesthetic motifs, the ring-in-ring metal complexes[7] have been utilized in templated synthesis of intricate Borromean rings.[8] Besides, the inclusion of a macrocycle within a macrocyclic host by noncovalent intermolecular forces, such as π-stacking,[9] hydrogen bonding,[10] metal coordination,[11] and hydrophobic interactions,[12] has been well-documented. Very recently, based on tetratopic ligand designs, supramolecular ring-in-ring[13] and sphere-in-sphere[13b,14] structures have been achieved. However, it still remains challenging to develop an efficient approach for expanding a ring-in-ring structure to next generation, for example, a well-defined ring-in-ring-in-ring superstructure. To this end, the involvement of multivalent ligands in the self-assembly process should be elucidated. Herein, we examined the multivalency[15] in our ligand design and carefully investigated the effect of linker length on the resultant self-assembled structures as well as their assembly mechanism. Through the fundamental understanding of self-assembly behavior of multivalent terpyridine ligands, a metallo-supramolecular trilayered ring (that is, a spiderweb structure) was successfully constructed in quantitative yield.

Hexakis(terpyridine) ligands **L**$^{1-3}$ (Scheme 1a) bearing alkyl linkers of various lengths (C4, C6, and C8) were synthesized by Pd-mediated coupling reactions of the corresponding aryl bromides with 4′-(4-boronophenyl)-tpy (where tpy = 2,2′:6′,2″-terpyridine) in good yields (59–93%), and their structures were confirmed by NMR spectroscopy and mass spectrometry (see the Supporting Information). Upon complexation of **L**^{1} with three molar equivalents of Cd^{II} ions at room temperature, the ^{1}H NMR spectrum (Figure 1b) showed three distinguishable sets of tpy resonances and a sharp singlet at 1.49 ppm assigned to the *tert*-butyl groups, suggesting the formation of discrete ring-in-ring structures.

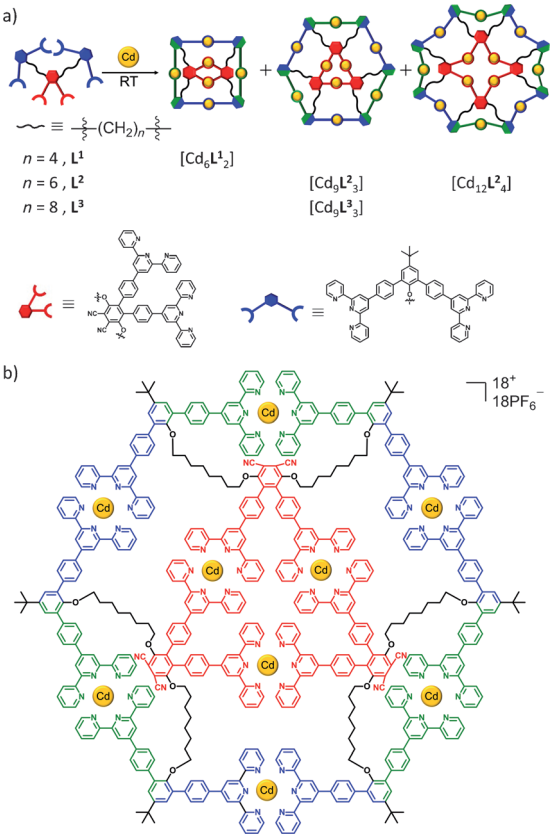

Scheme 1. a) Self-assembly of ring-in-ring structures from **L**^{1}, **L**^{2}, and **L**^{3}. b) The molecular structure of $[Cd_9L^3{}_3]$.

[*] J.-H. Fu, Y.-H. Lee, Y.-J. He, Prof. Dr. Y.-T. Chan
Department of Chemistry, National Taiwan University
No.1, Sec. 4, Roosevelt Rd., Taipei, 10617 (Taiwan)
E-mail: ytchan@ntu.edu.tw

[**] This research was supported by the Ministry of Science and Technology of Taiwan (NSC101-2113M-002-020-MY2 and MOST103-2113M-002-003-MY2). We gratefully thank Prof. Hao Ming Chen for TEM measurements.

Supporting information for this article is available on the WWW under http://dx.doi.org/10.1002/anie.201501507.

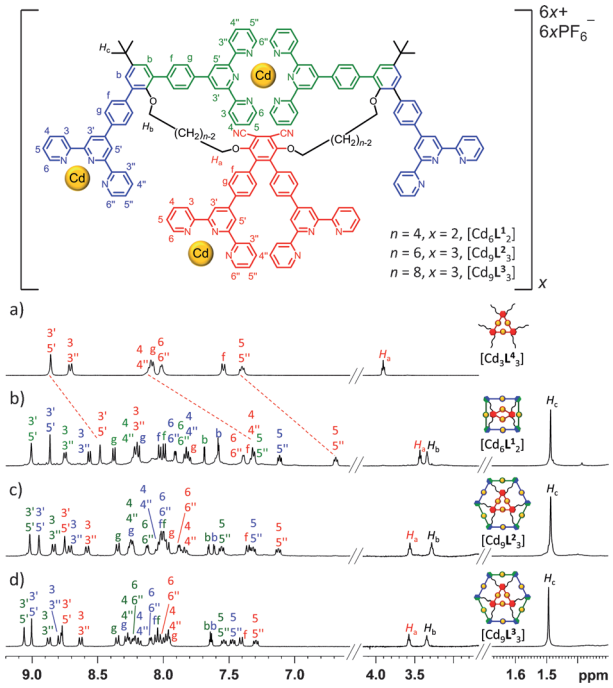

Figure 1. ^{1}H NMR spectra of a) $[Cd_3\mathbf{L}^{4}_3]$, b) $[Cd_6\mathbf{L}^{1}_2]$, c) $[Cd_9\mathbf{L}^{2}_3]$, and d) $[Cd_9\mathbf{L}^{3}_3]$.

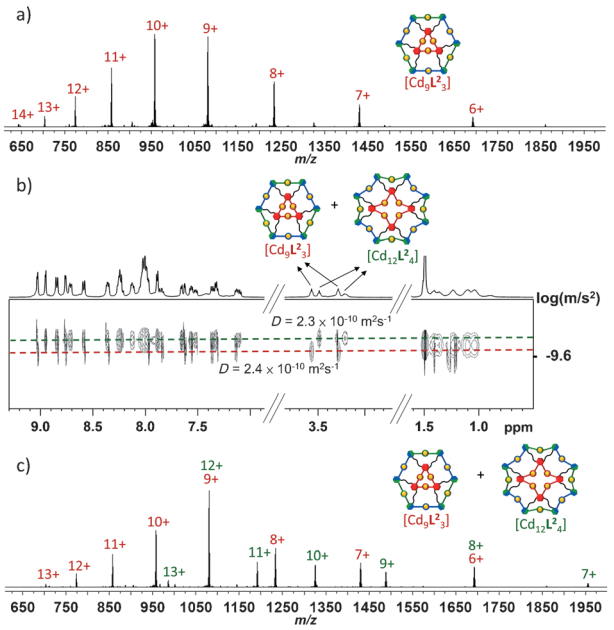

Figure 2. a) ESI-MS spectrum of $[Cd_9\mathbf{L}^{2}_3]$ ($[\mathbf{L}^{2}] = 7.5\times10^{-4}$ M). b) DOSY spectrum of a mixture of $[Cd_9\mathbf{L}^{2}_3]$ and $[Cd_{12}\mathbf{L}^{2}_4]$ ($[\mathbf{L}^{2}] = 6.0\times10^{-3}$ M). c) ESI-MS spectrum of a mixture of $[Cd_9\mathbf{L}^{2}_3]$ and $[Cd_{12}\mathbf{L}^{2}_4]$ ($[\mathbf{L}^{2}] = 6.0\times10^{-3}$ M). The charge states of $[Cd_9\mathbf{L}^{2}_3]$ and $[Cd_{12}\mathbf{L}^{2}_4]$ are shown in red and green, respectively.

The 2D COSY and ROESY NMR experiments (Supporting Information, Figure S17 and S18) were conducted to ensure the proper assignments. The diffusion-ordered spectroscopy (DOSY) NMR experiment (Supporting Information, Figure S16) indicated the existence of a single product (diffusion coefficient $D = 2.8\times10^{-10}$ m^{2}s^{-1}) in CD_3CN and the presence of $[Cd_6\mathbf{L}^{1}_2]$ was corroborated by the seven major ESI-MS peaks attributed to the ions with 4+ to 10+ charge states (Supporting Information, Figure S19). To confirm the unexpected structure, ligand $\mathbf{L}^{4}$ was synthesized and then complexed with Cd^{II} ions to give the triangular model complex $[Cd_3\mathbf{L}^{4}_3]$ (see the Supporting Information). The ^{1}H NMR resonances of $[Cd_6\mathbf{L}^{1}_2]$ for the central 60°-bent bis(terpyridine) motifs exhibited three significant upfield shifts for 3′,5′-tpy protons ($\delta = 8.48$ ppm, $\Delta\delta = -0.34$ ppm), 4,4″-tpy protons ($\delta = 7.32$ ppm, $\Delta\delta = -0.78$ ppm), and 5,5″-tpy protons ($\delta = 6.69$ ppm, $\Delta\delta = -0.71$ ppm) relative to those of $[Cd_3\mathbf{L}^{4}_3]$ (Figure 1a), strongly supporting that the inner ring is not a trimer but a dimer. Similar upfield shifts have been reported for the *o*-carborane-based metallomacrocyclic dimer and trimer.[16] Notably, no expected $[Cd_9\mathbf{L}^{1}_3]$ was formed, most likely as a result of the geometrical constraint caused by the short C4 linker. Molecular modeling (Supporting Information, Figure S55) revealed that the strain is estimated to increase the total energy by about 32 kcal mol^{-1} per repeat unit in $[Cd_9\mathbf{L}^{1}_3]$ as compared with $[Cd_6\mathbf{L}^{1}_2]$.

With a C6 linker, ligand $\mathbf{L}^{2}$ afforded the desired ring-in-ring structure $[Cd_9\mathbf{L}^{2}_3]$ upon coordination of Cd^{II} ions (3 equiv) at $[\mathbf{L}^{2}] = 7.5\times10^{-4}$ M, as evidenced by the ^{1}H NMR spectrum (Figure 1c) and the characteristic ESI-MS peaks (Figure 2a). However, the self-assembly composition was found to be concentration- and temperature-dependent. At higher ligand concentrations (above 1.5×10^{-3} M), another set of triplets at 3.48 and 3.21 ppm for the methylene units was clearly observed in the ^{1}H NMR spectrum (Supporting Information, Figure S20) and could be attributed to the tetramer⊂octamer $[Cd_{12}\mathbf{L}^{2}_4]$, which was further verified by its smaller diffusion coefficient of 2.3×10^{-10} m^{2}s^{-1} (Figure 2b) and by the distinctive ESI-MS peaks (Figure 2c). The proportion of $[Cd_{12}\mathbf{L}^{2}_4]$ was found to be increased with either increasing concentration or decreasing temperature (Supporting Information, Figure S21), indicating a dynamic equilibrium between $[Cd_9\mathbf{L}^{2}_3]$ and $[Cd_{12}\mathbf{L}^{2}_4]$.

Apparently, the supramolecular ring-in-ring architectures are significantly influenced by a subtle change in the linker length. Thus, to further investigate the linker effect, the Cd^{II} complex of $\mathbf{L}^{3}$ with a C8 linker was prepared in a similar manner. The ^{1}H, DOSY, and ^{113}Cd NMR spectra (Figure 1d; Supporting Information, Figures S31 and S35) as well as the ESI-MS (Figure 3a) analysis are in good agreement with the proposed ring-in-ring structure $[Cd_9\mathbf{L}^{3}_3]$ (Scheme 1b). The narrow drift time distributions for the 8+ to 16+ species observed in the ESI-TWIM-MS plot (Figure 3b) explicitly confirmed the absence of other isomers. Furthermore, the AFM image (Supporting Information, Figure S61) displayed an average height of 1.4 ± 0.1 nm, which is consistent with the modeled result.[17] However, the accuracy of the measured diameter (12.4 ± 0.7 nm) is very low, which is most likely due to the tip convolution effect.[18] The TEM image (Supporting Information, Figure S63) revealed an average diameter of 3.0 ± 0.4 nm, which is close to the distance (4.2 nm; Supporting Information, Figure S58) between two parallel sides of the geometry-optimized structure, providing additional evidence for the formation of the ring-in-ring structure. As compared

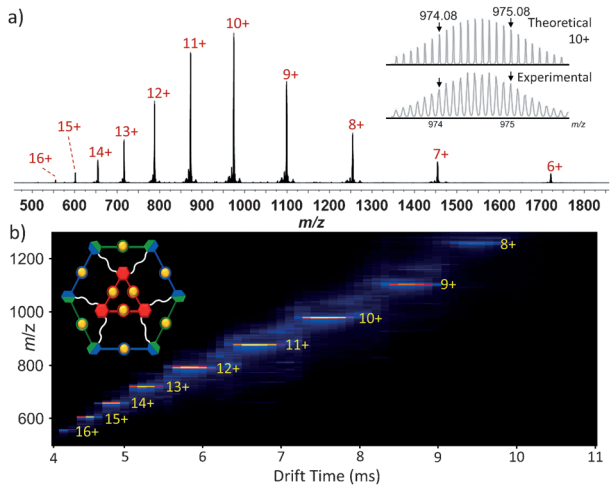

Figure 3. a) ESI-MS spectrum and b) ESI-TWIM-MS plot of $[Cd_9\mathbf{L}^3{}_3]$.

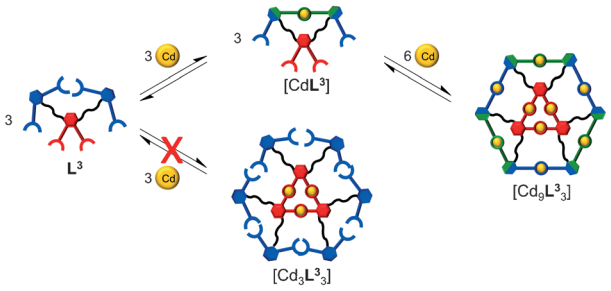

Scheme 2. A proposed formation mechanism for ring-in-ring $[Cd_9\mathbf{L}^3{}_3]$.

with $[Cd_9\mathbf{L}^2{}_3]$, $[Cd_9\mathbf{L}^3{}_3]$ was insensitive to concentration variations (Supporting Information, Figure S30), demonstrating that the lengthened linker successfully reduced the steric hindrance between the inner and outer macrocycles and shifted the equilibrium toward the predesigned ring-in-ring (tirmer⊂hexamer) structure.

Electrospray ionization interfaced with traveling-wave ion-mobility mass spectrometry (ESI-TWIM-MS)[19] was utilized to gain more structural insight into the ring-in-ring structures. The collision cross-sections (CCSs) derived from the corresponding drift times are consistent with the theoretical values obtained from the annealing simulation (Supporting Information, Tables S1–S3). For the relatively small and rigid structures, that is, $[Cd_6\mathbf{L}^1{}_2]$, $[Cd_9\mathbf{L}^2{}_3]$, and $[Cd_9\mathbf{L}^3{}_3]$, the CCSs do not vary much with charge. In contrast, a dramatic increase in the experimental CCS for $[Cd_{12}\mathbf{L}^2{}_4]$ was observed in higher charge states, which is supposedly due to the enhanced conformational flexibility[19e,20] in the lager tetramer⊂octamer structure (Supporting Information, Figure S57). Moreover, the computational result revealed two distinct conformers in the plot of calculated CCS versus relative energy (Supporting Information, Figure S60), supporting that $[Cd_{12}\mathbf{L}^2{}_4]$ is able to adopt an extended conformation to reduce charge repulsion and then gives rise to a larger CCS (1733.6 $Å^2$) for the 11+ ion.

To shed light on the formation mechanism for the ring-in-ring assembly, the titration experiment was conducted and monitored by ^{1}H NMR spectroscopy (Supporting Information, Figures S65–S67). The $[Cd(NO_3)_2]/[\mathbf{L}^3]$ ratio was increased from 0 to 3 at $[\mathbf{L}^3] = 3.0\times10^{-3}$ M. For the region of $0 \le [Cd(NO_3)_2]/[\mathbf{L}^3] \le 1$, only the 6,6″-tpy protons of 120°-bent bis(terpyridine)s were shifted significantly upfield, which is characteristic of octahedral tpy-Cd^{II}-tpy coordination,[21] and no obvious resonance change was found for the central 60°-bent ligand. An isosbestic point at 322 nm observed in the UV/Vis titration (Supporting Information, Figure S69b) further indicated the equilibrium between ligand $\mathbf{L}^3$ and intramolecularly complexed $[Cd\mathbf{L}^3]$. Moreover, the formation of $[Cd\mathbf{L}^3]$ was proved by ESI-MS (Supporting Information, Figure S68) and no peaks corresponding to $[Cd_3\mathbf{L}^3{}_3]$ (Scheme 2) were observed. For the region of $1 < [Cd(NO_3)_2]/[\mathbf{L}^3] \le 3$, the ^{1}H NMR spectra (Supporting Information, Figure S66) indicated that the concentration of $[Cd_9\mathbf{L}^3{}_3]$ (NO_3^- salt) increased proportionally to the added $[Cd(NO_3)_2]$ until reaching the equivalence point ($[Cd^{II}]/[\mathbf{L}^3] = 3$). The UV/Vis isosbestic point was slightly shifted to 314 nm (Supporting Information, Figure S69c) and the presence of $[Cd_9\mathbf{L}^3{}_3]$ was confirmed and tracked by ESI-MS (Supporting Information, Figure S68). In our original ligand design, we expected that the 60°-bent bis(terpyridine) ligands would give a stable triangle[22] as a template to induce the formation of a surrounding hexameric macrocycle. However, all the observations strongly suggested that instead of forming triangular $[Cd_3\mathbf{L}^3{}_3]$ with six dangling uncoordinated bis(terpyridine)s, $\mathbf{L}^3$ firstly undergoes intramolecular complexation to afford tetratopic $[Cd\mathbf{L}^3]$, which then cooperatively coordinates to Cd^{II} ions to produce the final ring-in-ring structure (Scheme 2).

Building on the understanding of self-assembly of ring-in-ring structures, we shifted our attention toward constructing a more complex supramolecular assembly, namely the spiderweb shown in Scheme 3, by extending the scaffold $\mathbf{L}^3$ horizontally along the linker axis. The multivalent ligand $\mathbf{L}^5$ was synthesized by the carbodiimide-mediated esterification of the corresponding dicarboxylic acid precursor and the subsequent Suzuki–Miyaura coupling at six aryl-bromo positions, and then purified by preparative gel permeation chromatography. It was expected that the elongated 120°-bent bis(terpyridine)s at the two ends could self-assemble into an enlarged hexamer to accommodate the inner ring-in-ring structure. When $\mathbf{L}^5$ was treated with five equivalents of Cd^{II} ions, the product gave broad ^{1}H NMR resonances (Supporting Information, Figure S41) in the aromatic region, which is presumably due to the conformational heterogeneity[23] of a giant complex. Nevertheless, one sharp ^{1}H NMR singlet at 1.50 ppm and two ^{13}C NMR resonances at 35.64 and 31.88 ppm (Supporting Information, Figures S41 and S42) corresponding to the *tert*-butyl markers suggested the formation of the expected spiderweb structure. The ^{1}H NMR assignments for the tpy moieties in five different chemical environments were carefully established by the COSY and ROESY spectra (Supporting Information, Figures S43–S47). In the DOSY spectrum (Supporting Information, Figure S40), the formation of a single assembly in CD_3NO_2 was evident from the diffusion coefficient of 1.1×10^{-10} m^2s^{-1} for all the relevant peaks. Furthermore, the fourteen prominent signals

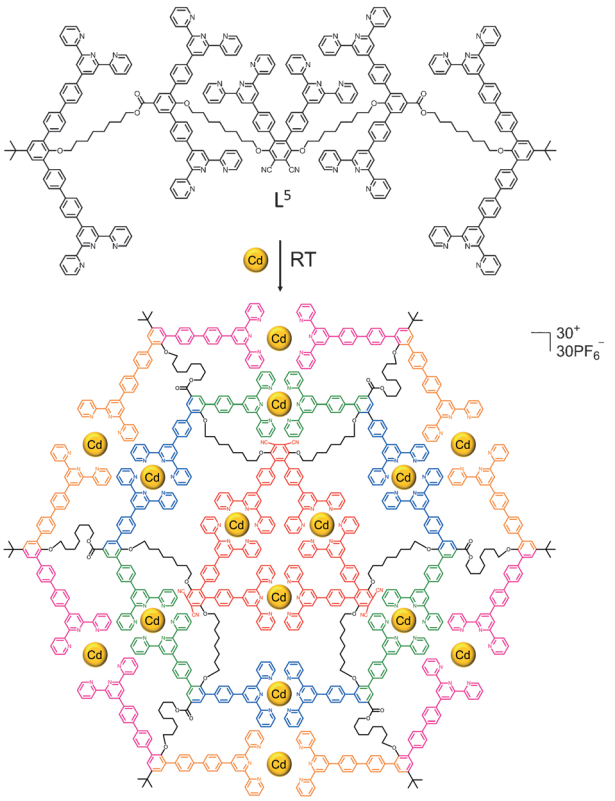

Scheme 3. Self-assembly of spiderweb $[Cd_{15}\mathbf{L}^{5}_{3}]$.

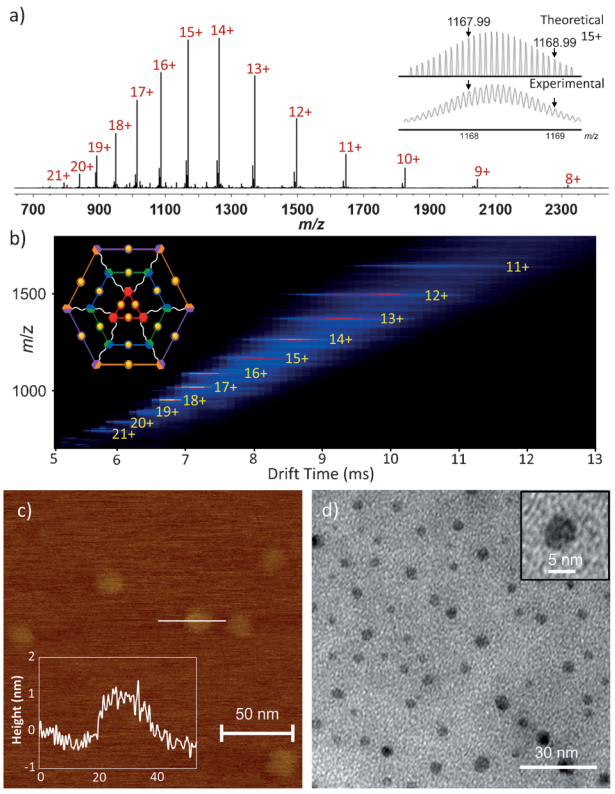

Figure 4. a) ESI-MS spectrum, b) ESI-TWIM-MS plot, c) AFM image, and d) TEM image of $[Cd_{15}\mathbf{L}^{5}_{3}]$.

generated from the 8+ to 21+ ions and their isotope patterns in the ESI-MS spectrum (Figure 4a; Supporting Information, Figure S39) unambiguously confirmed the assembled composition of $[Cd_{15}\mathbf{L}^{5}_{3}]$. The size analysis in gas phase conducted by ESI-TWIM-MS (Figure 4b) also revealed an average CCS of 2248.7 ± 100.3 Å^2, which is in good accord with the simulated results (Supporting Information, Table S4). The coin-like nanoplates of $[Cd_{15}\mathbf{L}^{5}_{3}]$ were visualized by AFM at a concentration of 1.0×10^{-8} M on mica (Figure 4c; Supporting Information, Figure S62). As mentioned previously, the average diameter (22.2 ± 0.7 nm) is not accurate, but larger than that of ring-in-ring $[Cd_{9}\mathbf{L}^{3}_{3}]$, whereas the measured height (1.1 ± 0.1 nm) agrees well with the dimension of a single tpy-Cd^{II}-tpy complex. A reasonable diameter of 5.0 ± 0.9 nm was finally observed by TEM imaging (Figure 4d).

In summary, the self-assembly of versatile metallo-supramolecular ring-in-ring structures has been successfully achieved by the complexation of Cd^{II} ions with the multivalent terpyridine ligands bearing different linker lengths. The flexible linker was found to be the key factor controlling the architecture and stability of the resultant assemblies, and the cooperative coordination of the tetratopic intermediate formed from intramolecular complexation facilitated the ring-in-ring formation. Based on the findings, the well-defined spiderweb structure was constructed as a demonstration of our design principle. We anticipate that this self-assembly process can provide facile access to construction of more sophisticated and functional supramolecular architectures.

Keywords: cadmium · multivalency · self-sorting · supramolecular chemistry · terpyridines

How to cite: *Angew. Chem. Int. Ed.* **2015**, *54*, 6231–6235
Angew. Chem. **2015**, *127*, 6329–6333

[1] H.-J. Schneider, *Applications of Supramolecular Chemistry*, CRC Press, Boca Raton, FL, **2012**.
[2] a) P. J. Stang, B. Olenyuk, *Acc. Chem. Res.* **1997**, *30*, 502–518; b) S. Leininger, B. Olenyuk, P. J. Stang, *Chem. Rev.* **2000**, *100*, 853–908; c) R. Chakrabarty, P. S. Mukherjee, P. J. Stang, *Chem. Rev.* **2011**, *111*, 6810–6918.
[3] G. R. Newkome, C. N. Moorefield, *Chem. Soc. Rev.* **2015**. DOI: 10.1039/C4CS00234B.
[4] a) K. Harris, D. Fujita, M. Fujita, *Chem. Commun.* **2013**, *49*, 6703–6712; b) A. M. Castilla, W. J. Ramsay, J. R. Nitschke, *Acc. Chem. Res.* **2014**, *47*, 2063–2073.
[5] a) J. M. Lehn, A. Rigault, J. Siegel, J. Harrowfield, B. Chevrier, D. Moras, *Proc. Natl. Acad. Sci. USA* **1987**, *84*, 2565–2569; b) B. Hasenknopf, J.-M. Lehn, B. O. Kneisel, G. Baum, D. Fenske, *Angew. Chem. Int. Ed. Engl.* **1996**, *35*, 1838–1840; *Angew. Chem.* **1996**, *108*, 1987–1990; c) M. Albrecht, *Chem. Rev.* **2001**, *101*, 3457–3498.
[6] J. E. Beves, B. A. Blight, C. J. Campbell, D. A. Leigh, R. T. McBurney, *Angew. Chem. Int. Ed.* **2011**, *50*, 9260–9327; *Angew. Chem.* **2011**, *123*, 9428–9499.
[7] J. C. Loren, M. Yoshizawa, R. F. Haldimann, A. Linden, J. S. Siegel, *Angew. Chem. Int. Ed.* **2003**, *42*, 5702–5705; *Angew. Chem.* **2003**, *115*, 5880–5883.
[8] R. S. Forgan, J.-P. Sauvage, J. F. Stoddart, *Chem. Rev.* **2011**, *111*, 5434–5464.
[9] a) T. Kawase, Y. Nishiyama, T. Nakamura, T. Ebi, K. Matsumoto, H. Kurata, M. Oda, *Angew. Chem. Int. Ed.* **2007**, *46*, 1086–

1088; *Angew. Chem.* **2007**, *119*, 1104 – 1106; b) R. S. Forgan, D. C. Friedman, C. L. Stern, C. J. Bruns, J. F. Stoddart, *Chem. Commun.* **2010**, *46*, 5861 – 5863.
[10] a) S.-H. Chiu, A. R. Pease, J. F. Stoddart, A. J. P. White, D. J. Williams, *Angew. Chem. Int. Ed.* **2002**, *41*, 270 – 274; *Angew. Chem.* **2002**, *114*, 280 – 284; b) A. Tsuda, E. Hirahara, Y.-S. Kim, H. Tanaka, T. Kawai, T. Aida, *Angew. Chem. Int. Ed.* **2004**, *43*, 6327 – 6331; *Angew. Chem.* **2004**, *116*, 6487 – 6491.
[11] a) S. Anderson, H. L. Anderson, A. Bashall, M. McPartlin, J. K. M. Sanders, *Angew. Chem. Int. Ed. Engl.* **1995**, *34*, 1096 – 1099; *Angew. Chem.* **1995**, *107*, 1196 – 1200; b) M. Schmittel, A. Ganz, D. Fenske, *Org. Lett.* **2002**, *4*, 2289 – 2292.
[12] a) S.-Y. Kim, I.-S. Jung, E. Lee, J. Kim, S. Sakamoto, K. Yamaguchi, K. Kim, *Angew. Chem. Int. Ed.* **2001**, *40*, 2119 – 2121; *Angew. Chem.* **2001**, *113*, 2177 – 2179; b) A. I. Day, R. J. Blanch, A. P. Arnold, S. Lorenzo, G. R. Lewis, I. Dance, *Angew. Chem. Int. Ed.* **2002**, *41*, 275 – 277; *Angew. Chem.* **2002**, *114*, 285 – 287; c) Y. Liu, *Tetrahedron Lett.* **2007**, *48*, 3871 – 3874.
[13] a) M. Wang, C. Wang, X.-Q. Hao, J. Liu, X. Li, C. Xu, A. Lopez, L. Sun, M.-P. Song, H.-B. Yang, X. Li, *J. Am. Chem. Soc.* **2014**, *136*, 6664 – 6671; b) B. Sun, M. Wang, Z. Lou, M. Huang, C. Xu, X. Li, L.-J. Chen, Y. Yu, G. L. Davis, B. Xu, H.-B. Yang, X. Li, *J. Am. Chem. Soc.* **2015**, *137*, 1556 – 1564.
[14] Q.-F. Sun, T. Murase, S. Sato, M. Fujita, *Angew. Chem. Int. Ed.* **2011**, *50*, 10318 – 10321; *Angew. Chem.* **2011**, *123*, 10502 – 10505.
[15] a) M. Mammen, S.-K. Choi, G. M. Whitesides, *Angew. Chem. Int. Ed.* **1998**, *37*, 2754 – 2794; *Angew. Chem.* **1998**, *110*, 2908 – 2953; b) C. Fasting, C. A. Schalley, M. Weber, O. Seitz, S. Hecht, B. Koksch, J. Dernedde, C. Graf, E.-W. Knapp, R. Haag, *Angew. Chem. Int. Ed.* **2012**, *51*, 10472 – 10498; *Angew. Chem.* **2012**, *124*, 10622 – 10650.
[16] J. M. Ludlow III, M. Tominaga, Y. Chujo, A. Schultz, X. Lu, T. Xie, K. Guo, C. N. Moorefield, C. Wesdemiotis, G. R. Newkome, *Dalton Trans.* **2014**, *43*, 9604 – 9611.
[17] T. Bauer, Z. Zheng, A. Renn, R. Enning, A. Stemmer, J. Sakamoto, A. D. Schlüter, *Angew. Chem. Int. Ed.* **2011**, *50*, 7879 – 7884; *Angew. Chem.* **2011**, *123*, 8025 – 8030.
[18] a) M. Radmacher, M. Fritz, H. Hansma, P. Hansma, *Science* **1994**, *265*, 1577 – 1579; b) A. A. Bukharaev, N. V. Berdunov, D. V. Ovchinnikov, K. M. Salikhov, *Scanning Microsc.* **1998**, *12*, 225 – 234; c) C.-F. Josep, C. Eugenio, F.-A. Alicia, P.-C. Elena, *Nanotechnology* **2014**, *25*, 395703.
[19] a) Y.-T. Chan, X. Li, M. Soler, J.-L. Wang, C. Wesdemiotis, G. R. Newkome, *J. Am. Chem. Soc.* **2009**, *131*, 16395 – 16397; b) E. R. Brocker, S. E. Anderson, B. H. Northrop, P. J. Stang, M. T. Bowers, *J. Am. Chem. Soc.* **2010**, *132*, 13486 – 13494; c) Y.-T. Chan, X. Li, J. Yu, G. A. Carri, C. N. Moorefield, G. R. Newkome, C. Wesdemiotis, *J. Am. Chem. Soc.* **2011**, *133*, 11967 – 11976; d) J. Ujma, M. De Cecco, O. Chepelin, H. Levene, C. Moffat, S. J. Pike, P. J. Lusby, P. E. Barran, *Chem. Commun.* **2012**, *48*, 4423 – 4425; e) F. Lanucara, S. W. Holman, C. J. Gray, C. E. Eyers, *Nat. Chem.* **2014**, *6*, 281 – 294.
[20] Y.-T. Chan, X. Li, C. N. Moorefield, C. Wesdemiotis, G. R. Newkome, *Chem. Eur. J.* **2011**, *17*, 7750 – 7754.
[21] U. S. Schubert, A. Winter, G. R. Newkome, *Terpyridine-Based Materials*, Wiley-VCH, Weinheim, **2011**, pp. 65 – 127.
[22] A. Schultz, Y. Cao, M. Huang, S. Z. D. Cheng, X. Li, C. N. Moorefield, C. Wesdemiotis, G. R. Newkome, *Dalton Trans.* **2012**, *41*, 11573 – 11575.
[23] Q.-F. Sun, J. Iwasa, D. Ogawa, Y. Ishido, S. Sato, T. Ozeki, Y. Sei, K. Yamaguchi, M. Fujita, *Science* **2010**, *328*, 1144 – 1147.

Received: February 16, 2015
Published online: April 7, 2015

